PROCEEDINGS, Nineteenth Workshop on Geothermal Reservoir Engineering
Stanford University, Stanford, California, January 18-20, 1994
SGP-TR-147

FLOW NEAR THE CRITICAL POINT: EXAMINATION OF SOME PRESSURE-ENTHALPY PATHS

Daniel O. Hayba[1] and Steven E. Ingebritsen[2]

[1]MS 959, U.S. Geological Survey, Reston, VA 22092
[2]MS 439, U.S. Geological Survey, Menlo Park, CA 94025

ABSTRACT

Quantitative flow modeling of fluids at elevated temperatures and pressures has generally been limited to consideration of either single-phase flow or two-phase flow at conditions below the critical point of water. In this paper, we introduce a version of the GEOTHER model that can simulate both multiphase flow and flow above the critical point, and demonstrate its capabilities by simulating flow in the vicinity of the critical point. GEOTHER2 is a multiphase, finite-difference model that simulates three-dimensional flow of pure water and heat at temperatures ranging from 0° to 1,200°C and pressures ranging from 0.5 to 10,000 bars. The governing equations are expressions of mass and energy conservation that are posed in terms of pressure and enthalpy. A series of one-dimensional experiments indicates that permeability is a pivotal factor in determining pressure-enthalpy/temperature trajectories near the critical point. At low permeabilities ($\leq 10^{-18}$ m^2), heat transport by conduction dominates, and the trajectory defines a constant thermal gradient. At higher permeabilities ($\geq 10^{-16}$ m^2), advective heat transport dominates, and the pressure-enthalpy trajectory maintains a constant "flowing enthalpy".

INTRODUCTION

Transport processes in magmatic-hydrothermal systems involve single- or two-phase flow of fluids at temperatures ranging from 0° to >1,000°C and pressures ranging up to several kilobars. The properties of water vary substantially over this P-T range, especially in the vicinity of the critical point, where some fluid properties exhibit extrema. Although these near-critical extrema may influence flow patterns in hydrothermal systems, computational difficulties have inhibited quantitative modeling of flow near the critical point. In this paper, we introduce an extended version of the computer program GEOTHER that is capable of simulating near-critical flow, and demonstrate this capability with some one-dimensional, steady-state experiments.

In the past, most users of geothermal models have had to choose between models for multiphase, pure-water (or water and gas) systems with a temperature range of about 0-350°C, and models for single-phase pure-water systems with a temperature range of about 0-1,000°C. Most of the multiphase, subcritical models were designed by reservoir-engineering groups to handle the range of conditions encountered in geothermal-reservoir development (e.g. TOUGH2: Pruess, 1991), whereas most of the single-phase, high-temperature models were developed by geoscience groups to examine heat transfer associated with cooling plutons (e.g. Norton and Knight, 1977; Cathles, 1977). Both types of models have generally assumed that the circulating fluid is pure water or water and noncondensible gas, although Battistelli and others (in press) recently presented a solute-transport algorithm for the TOUGH2 simulator.

One of the major obstacles to the development of a more complete geothermal model has been the radical variation in fluid properties near the critical point. For simulators that use pressure and temperature as dependent variables, the critical point poses particularly difficult problems. In P-T coordinates, the critical point is at the vertex of the vaporization curve and is a singularity in equations of state. For example, the partial derivatives of $\rho(P,T)$ diverge to positive and negative infinity, and $C_v(P,T)$ diverges to infinity (see, e.g., Johnson and Norton, 1991).

Multiphase models cannot use a pressure-temperature formulation because a P-T pair does not specify saturation. Some multiphase codes, such as TOUGH2 (Pruess, 1991), switch variables, solving for pressure and temperature in the single-phase region and pressure and saturation in the two-phase region. In developing the original version of GEOTHER, Faust and Mercer (1977, 1979a) took a different approach, choosing pressure and enthalpy as dependent variables because they uniquely specify the thermodynamic state of the fluid under both single-and two-phase conditions (fig. 1). This choice of variables greatly facilitated the extension of GEOTHER to supercritical conditions, because the pressure-enthalpy formulation eliminates singularities at the critical point.

THE GEOTHER2 MODEL

GEOTHER2 is a three-dimensional, finite-difference model that can simulate both multiphase and supercritical flow of pure water and heat in a porous medium. This program is a descendent of the models developed at the U.S. Geological Survey by Faust and Mercer (1977, 1979a, 1979b, 1982). We have modified the 1982 version of the program by extending the temperature range to 0-1,200°C and the pressure range to 0.5-10,000 bars, modularizing the program architecture, adding provisions for spatial and temporal variation of porous-medium properties, automating the time-step control, making the convergence criteria more rigorous, and extensively revising the input and output formats. We have made only relatively minor changes to the mathematical model and

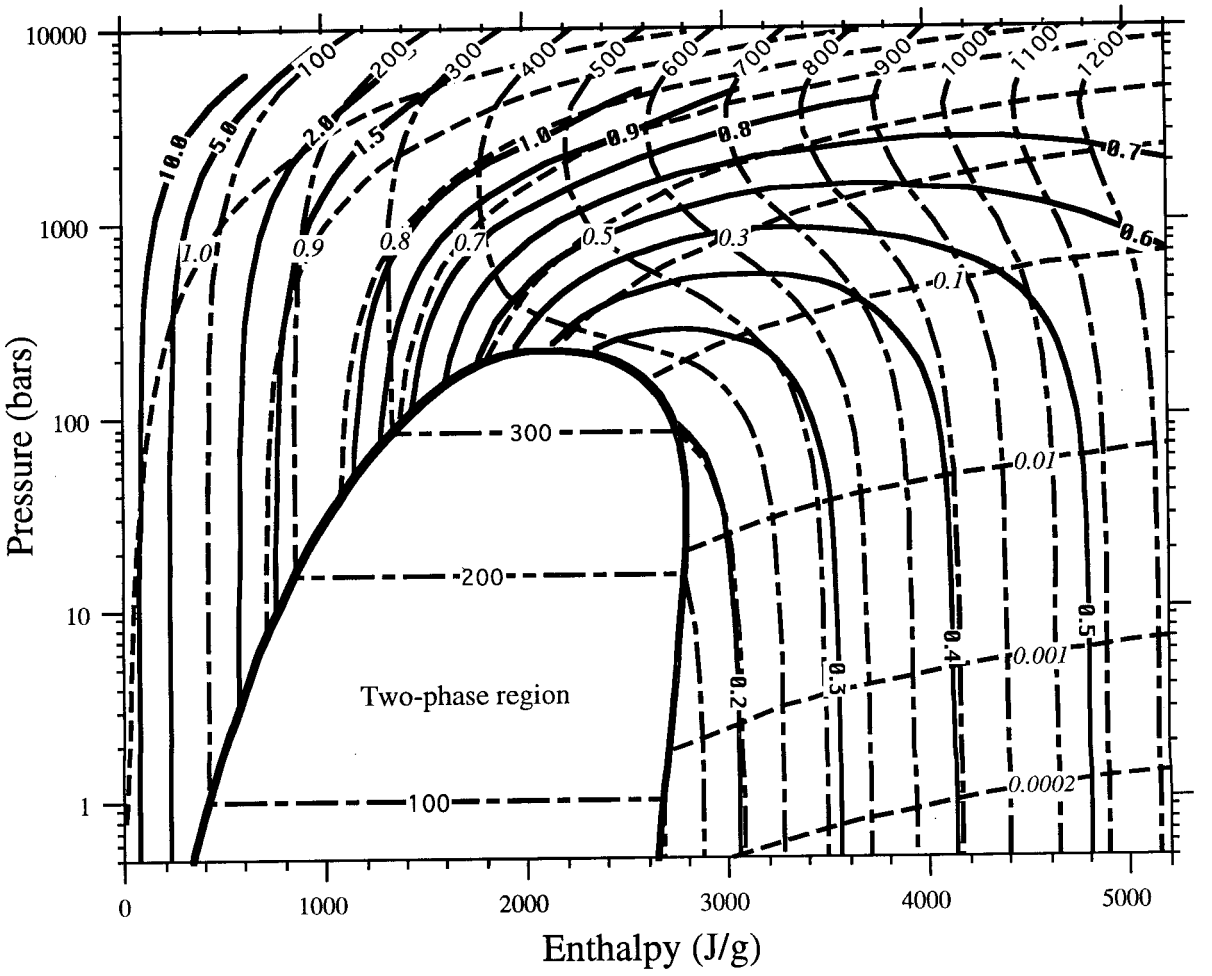

*Figure 1. Pressure-enthalpy diagram for pure water, showing contours of equal temperature, density, and viscosity. Saturated enthalpies of steam and liquid water define the boundaries of the two-phase region, and meet at the critical point (220.55 bars and 2086.0 J/g). Temperatures (*100*, long dashed lines) in °C; densities (0.02, short dashed lines) in g/cm^3; and viscosities (*0.2*, solid lines) in g/cm/sec x 10^{-3}.*

solution algorithm described by Faust and Mercer (1979a, 1979b, 1982). A complete documentation of GEOTHER2 is undergoing internal review at the U.S. Geological Survey. Ingebritsen (1986) and Hayba (1993) summarized earlier improvements to the Faust and Mercer (1982) version of GEOTHER, and Roberts and others (1987) described another extended version (to 1,000°C and 1 kbar) of the Faust and Mercer model that has not entered the public domain.

The governing equations for GEOTHER2 are expressions of mass and energy conservation, posed in terms of pressure and enthalpy:

$$\frac{\partial}{\partial t}\left[\phi(S_w\rho_w+(1-S_w)\rho_s)\right] - \nabla\cdot\left[\frac{\mathbf{k}k_{rs}\rho_s}{\mu_s}\cdot(\nabla P-\rho_s g\nabla D)\right] - \nabla\cdot\left[\frac{\mathbf{k}k_{rw}\rho_w}{\mu_w}\cdot(\nabla P-\rho_w g\nabla D)\right]-(R_s+R_w)=0 \qquad (1)$$

and

$$\frac{\partial}{\partial t}\left[\phi(S_w\rho_w H_w+(1-S_w)\rho_s H_s)+(1-\phi)\rho_r H_r\right] - \nabla\cdot\left[\frac{\mathbf{k}k_{rs}\rho_s H_s}{\mu_s}\cdot(\nabla P-\rho_s g\nabla D)\right] - \nabla\cdot\left[\frac{\mathbf{k}k_{rw}\rho_w H_w}{\mu_w}\cdot(\nabla P-\rho_w g\nabla D)\right] - \nabla\cdot\left[K_m T\right]-(R_s H_s+R_w H_w)=0 \qquad (2)$$

There are also several constitutive relations that complete the description of the system. Faust and Mercer (1979a) discuss these relations and various assumptions implicit in the governing equations. The more important assumptions are that a two-phase form of Darcy's Law is valid; capillary-pressure effects are negligible; rock and water are in thermal equilibrium; and heat transfer by dispersion and radiation are negligible.

The mass- and energy-balance equations are strongly coupled and highly nonlinear, because a number of the independent variables are functions of the dependent variables. The relative permeabilities, densities, and viscosities, in particular, vary widely with pressure and enthalpy. GEOTHER2 uses Newton-Raphson iteration to treat these nonlinear coefficients, and solves each vertical cross section of the finite-difference grid implicitly. For three-dimensional models, the solution technique is slice-successive overrelaxation embedded in the Newton-Raphson iteration. Convergence of the Newton-Raphson technique is determined by checking mass and energy balances for each finite-difference block.

The regression equations for fluid densities, viscosities, and temperature that were used in earlier versions of GEOTHER are accurate over the temperature range 10 - 300°C. We replaced these equations with an extended (0 - 1,200°C) lookup table that is interrogated by a bicubic interpolation routine. This method, which is accurate and relatively fast, provides values for density, viscosity, and temperature as well as the gradients of those values with respect to pressure and enthalpy. However, the table is large, containing approximately 4,500 grid points (P-H pairs), and requires about 2 Mbytes of space in binary form. The fluid density and temperature values in the lookup table are from the routines of Haar and others (1984), and the viscosity values are from the formulation by Watson and others (1980), which Sengers and Kamgar-Parsi (1984) re-evaluated using density values of Haar and others (1984). Although we applied the viscosity equation beyond its valid range (≤5 kbar and ≤900°C), we expect that the error introduced by this extrapolation is relatively modest. For the two-phase region, we use cubic splines to describe the saturated-water and saturated-steam curves. These splines provide values for the enthalpy, density, temperature, and viscosity of saturated liquid water and steam as functions of pressure.

Extending GEOTHER beyond the critical point created some problems with the definition of volumetric saturation and the liquid water/steam nomenclature. Above the critical point, the distinction between liquid and steam disappears, and the values assigned to the saturation variables become arbitrary. However, below the critical point, saturation is an important variable, and computational problems can arise in determining the average fluid properties for flow between super- and subcritical blocks. We enforced consistent averaging by treating supercritical blocks as though they contain two phases with identical properties (density, viscosity, saturation, and relative permeability).

PREVIOUS WORK ON NEAR-CRITICAL FLOW

Norton and Knight (1977) were among the first to suggest that variations in fluid properties near the critical point of water may influence transport in magmatic-hydrothermal systems. They recognized that near-critical maxima in thermal expansivity and heat capacity nearly coincide with a minima in kinematic viscosity, thereby maximizing buoyancy forces and heat-transport capacity while minimizing viscous-drag forces. They further suggested that the near-critical extrema in fluid properties may control the overall style of fluid circulation, while noting that small differential pressure and temperature values would be required to adequately simulate the process, because the greatest variation in fluid properties occurs over a narrow P-T range. Johnson and Norton (1991) presented complete equations of state for pure water in the critical region and reiterated the importance of near-critical fluid properties to flow in hydrothermal systems, but did not simulate flow and transport.

Dunn and Hardee (1981) conducted laboratory experiments on heat-transfer enhancement in the vicinity of the critical point. Their experiments involved a heated platinum wire in the center of a cylindrical vessel filled with water-saturated silica sand. They applied constant current to the wire while maintaining the vessel wall at constant temperature. At pressures slightly above the critical point, they measured the energy required to establish a small temperature difference (~2°C) within the vessel. They suggested that their experimental results indicate near-critical heat-transfer rates as much as 70 times greater than conductive rates at ambient temperatures.

Cox and Pruess (1990), using an extended version of the TOUGH2 simulator, attempted to simulate the Dunn and Hardee (1981) experiments numerically, and found heat-

Table 1. Mass and energy fluxes from one-dimensional simulations in the vicinity of the critical point

	Permeability (m^2)	Mass flux ($g/s/m^2$)	Energy flux (W/m^2)
Set 1.	Flow from 240.55 bars, 1886 J/g to 200.55 bars, 1886 J/g		
	10^{-20}	4.0×10^{-7}	2.0×10^{-2}
	10^{-18}	3.5×10^{-5}	8.4×10^{-2}
	10^{-16}	3.5×10^{-3}	6.5
	10^{-14}	3.5×10^{-1}	6.5×10^{2}
Set 2.	Flow from 240.55 bars, 2086 J/g to 200.55 bars, 2086 J/g		
	10^{-20}	3.6×10^{-7}	3.1×10^{-2}
	10^{-18}	3.3×10^{-5}	9.7×10^{-2}
	10^{-16}	3.2×10^{-3}	6.7
	10^{-14}	3.2×10^{-1}	6.7×10^{2}
Set 3.	Flow from 240.55 bars, 2286 J/g to 200.55 bars, 2286 J/g		
	10^{-20}	2.7×10^{-7}	3.5×10^{-2}
	10^{-18}	2.8×10^{-5}	1.0×10^{-1}
	10^{-16}	2.8×10^{-3}	6.5
	10^{-14}	2.8×10^{-1}	6.5×10^{2}
Set 4.	Flow from 230.55 bars, 2086 J/g to 210.55 bars, 1786 J/g		
	10^{-20}	2.9×10^{-7}	2.6×10^{-2}
	10^{-18}	1.7×10^{-5}	5.8×10^{-2}
	10^{-16}	1.6×10^{-3}	3.4
	10^{-14}	1.6×10^{-1}	3.4×10^{2}
Set 5.	Flow from 240.55 bars, 268 J/g to 200.55 bars, 1486 J/g		
	10^{-20}	3.0×10^{-7}	1.6×10^{-1}
	10^{-18}	2.8×10^{-5}	2.1×10^{-1}
	10^{-16}	2.0×10^{-3}	5.4
	10^{-14}	1.9×10^{-1}	5.2×10^{2}

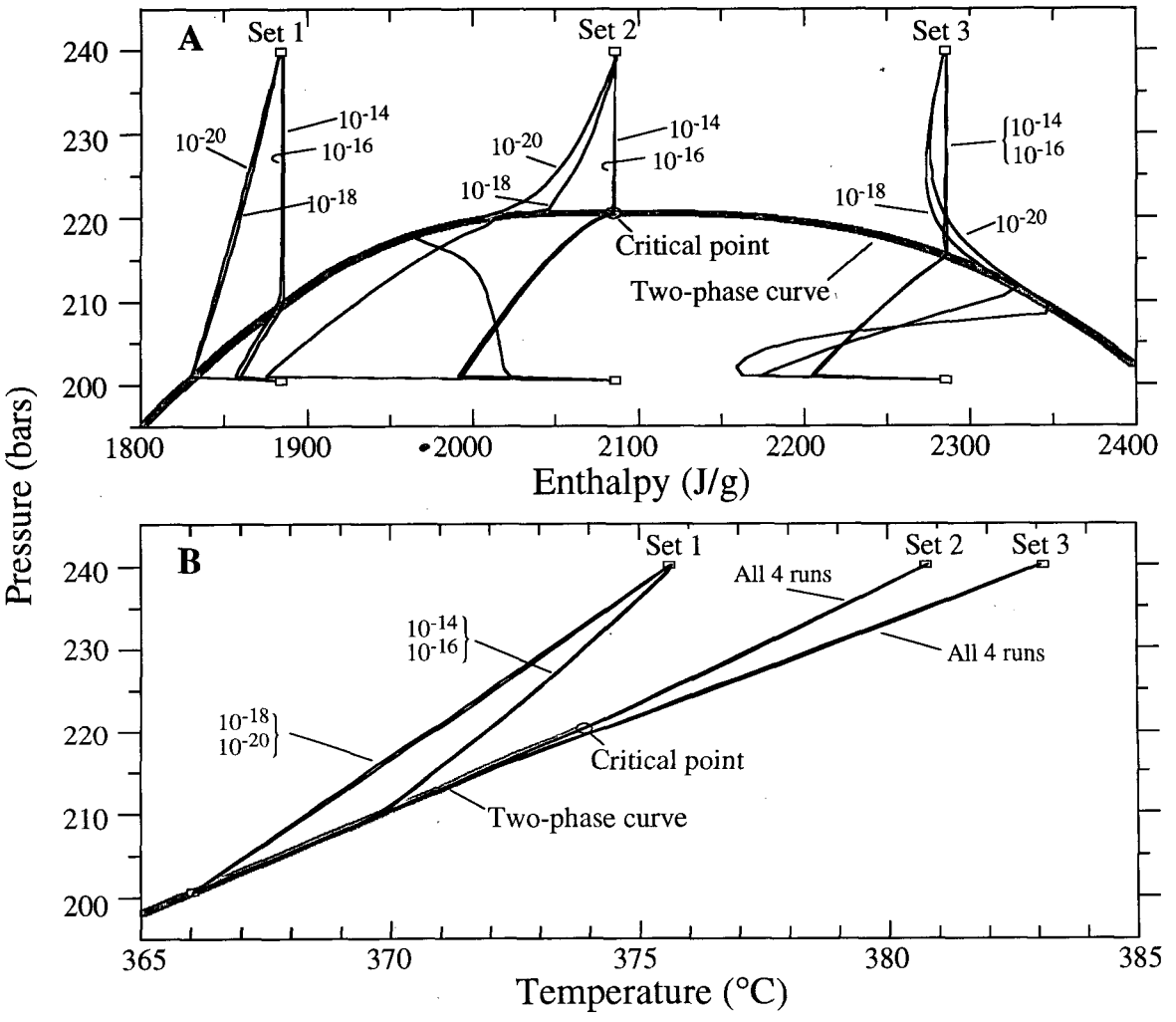

Figure 2. A, Pressure-enthalpy and B, pressure-temperature trajectories for three sets of one-dimensional experiments in which both endpoints of the column were held at the same enthalpy (see table 1).

transfer enhancement over a temperature range of about 40°C, whereas the numerical simulations and a Rayleigh Number analysis suggested large enhancements over only a 2-3°C temperature interval. We have not tried to simulate the Dunn and Hardee (1981) experiments, but we do have some preliminary results for a two-dimensional (10 m x 10 m) vertical slab with comparable permeability ($2x10^{-12}$ m^2), pressure (221 bars), and temperature difference (2°C). Our simulations show heat transfer enhancements of >100 for a narrow temperature interval bracketing the critical point.

NEAR-CRITICAL PRESSURE-ENTHALPY PATHS

The numerical results from GEOTHER2 reported here illustrate some of the factors controlling fluid trajectories in the critical region. Our approach was to assign constant pressure and enthalpy values (table 1) at either end of a 1-km-long horizontal column divided into 25-m blocks. We varied the permeability of the column but held thermal conductivity constant at 2 W/m K. Arbitrary initial conditions were assigned to the interior of the column and equations (1) and (2) were solved iteratively until mass and energy fluxes reached a steady state, i.e., until mass and energy entering the high P-H end of the column equated with mass and energy exiting at the low P-H end. These one-dimensional experiments do not allow us to address the issue of enhanced convective heat transfer, but are a useful test case.

Figure 2 shows the results of three sets of experiments in which we assigned the same enthalpy values, but different pressure values, at either end of the column. Thus the endpoints define vertical lines in P-H coordinates. Within each set, differences in permeability cause the flow path to take different trajectories that are much more distinguishable in P-H coordinates (fig. 2A) than in P-T coordinates (fig. 2B). Each set involves a fixed pressure drop of 40 bars, and within each set mass and energy fluxes scale nearly linearly with permeability (table 1). The fluxes associated with the high-permeability ($\geq 10^{-16}$ m^2) experiments which pass through the critical point (table 1, set 2) do not appear to be significantly larger than the fluxes obtained in high-permeability experiments which bypass the critical point (table 1, sets 1 and 3). Constant P-H boundaries more tightly focused on the critical point may be needed to define any enhancements in transport.

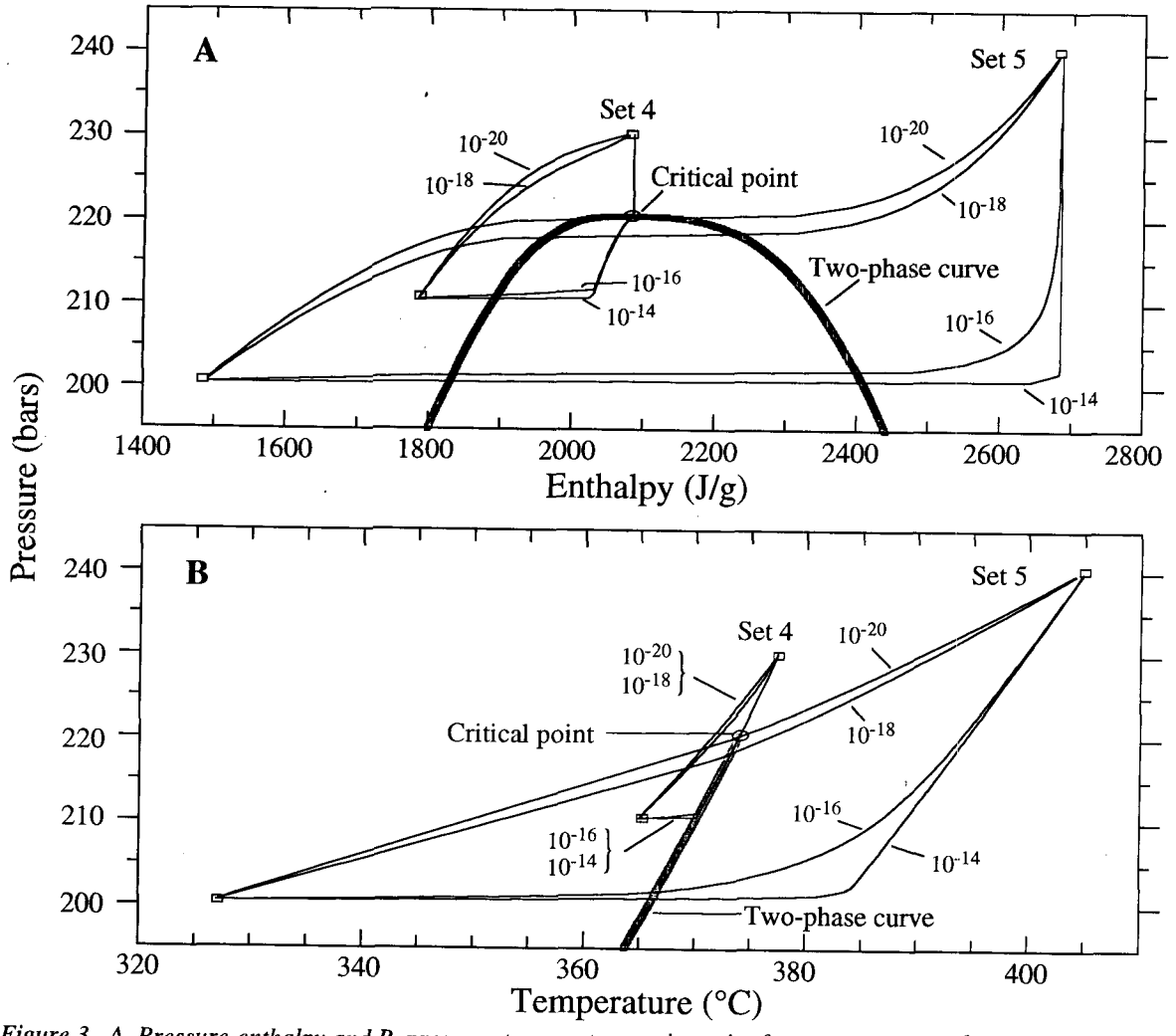

Figure 3. A, Pressure-enthalpy and B, pressure-temperature trajectories for two sets of one-dimensional experiments in which the endpoints of the column were held at different pressures and enthalpies (see table 1).

In other sets of experiments, designated sets 4 and 5 (fig. 3), we assigned different values of enthalpy and pressure at either end of the column, so that the end points define diagonals in P-H coordinates. In set 4, the high-permeability experiments intersect the critical point, whereas in set 5 the low-permeability runs do so. These two sets of experiments also highlight the importance of permeability in determining the trajectory of the flow path. Figure 4 shows the temperature gradient along the column for the set 4 experiments, and figure 5 shows the "flowing enthalpy", which is

$$H_{FLOWING} = \left(v_w \rho_w H_w + v_s \rho_s H_s\right) / \left(v_w \rho_w + v_s \rho_s\right) \quad (3)$$

In single-phase regions, flowing enthalpy is identical to the enthalpy of the fluid in place, but in the two-phase region the two enthalpy values are often significantly different.

At low permeabilities ($\leq 10^{-18}$ m^2), heat transport by conduction dominates, and the P-H and P-T trajectories (fig. 3) define a constant temperature gradient (fig. 4). At higher permeabilities ($\geq 10^{-16}$ m^2) advection dominates, and the cooling trajectories (fig. 3) reflect a nearly constant flowing enthalpy along the flow path (fig. 5). The transition from conduction- to advection-dominated transport seen at permeabilities between 10^{-18} m^2 and 10^{-16} m^2 is consistent with Norton and Knight's (1977) estimate. In the high-permeability cases, most of the variation in temperature gradient and flowing enthalpy occurs near the outflow boundary, where the lower enthalpy/temperature specified at that boundary must finally be accommodated. Analytical solutions for steady flow between constant-temperature boundaries (Bredehoeft and Papadopolous, 1965) predict similarly sharp variations for comparable flow rates. These sharp variations in enthalpy near the constant (H, P) outflow boundary disappeared when we reran these experiments with constant-flux outflow boundaries, specifying the mass fluxes determined from the runs with constant value boundaries (table 1). The results with constant-flux outflow boundaries were otherwise identical to the results with the constant (H,P) outflow boundaries.

In single-phase regions, the advection-dominated trajectories are essentially isoenthalpic (figs. 2 and 3). In the two-phase region, the flowing enthalpy is strongly

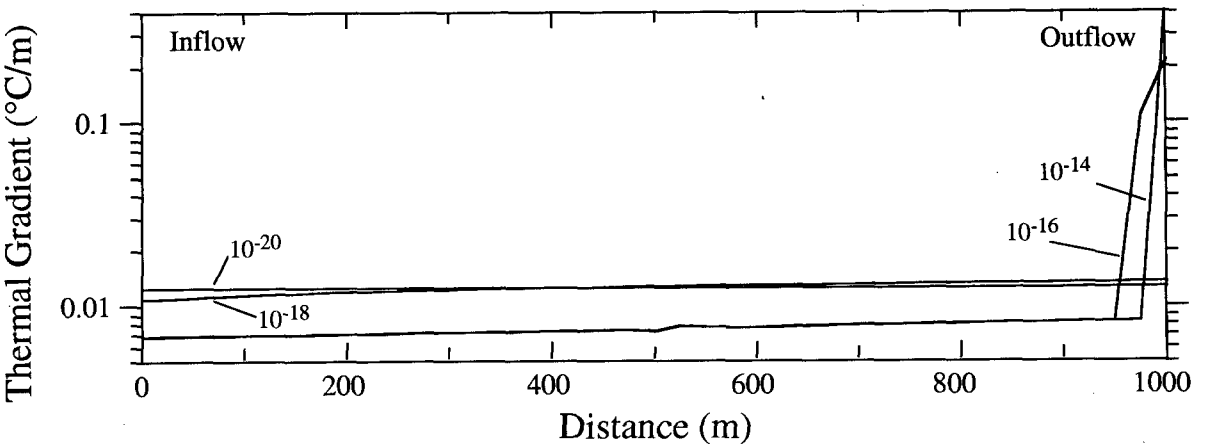

Figure 4. Results from set 4 experiments, showing relation between temperature gradient and distance along column for selected permeability values. See figure 3 for associated pressure-enthalpy and pressure- temperature trajectories.

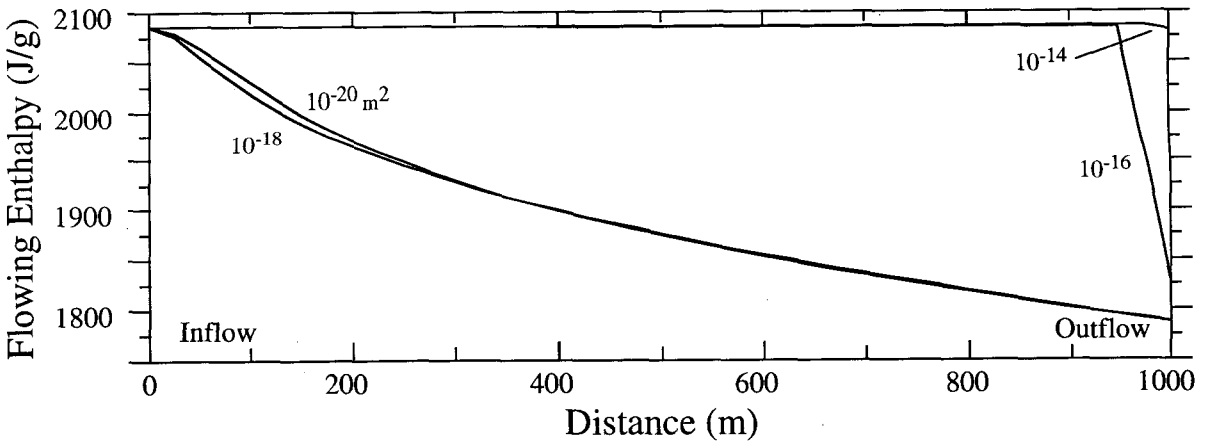

Figure 5. Results from set 4 experiments, showing relation between flowing enthalpy and distance along column for selected permeability values. See figure 3 for associated pressure-enthalpy and pressure-temperature trajectories, and figure 4 for thermal gradients.

dependent on the mobilities of the two phases; therefore, the choice of relative permeability functions affects the pressure-enthalpy trajectories. We used simple linear functions with no residual liquid or steam saturation to obtain the results shown here. Because advection-dominated pressure-enthalpy trajectories are dictated by the requirement of maintaining a constant flowing enthalpy, using different relative-permeability functions and/or non-zero residual saturations would change the trajectories of the high-permeability experiments through the two-phase region. In that sense, the particular trajectories shown in Figures 2 and 3 are arbitrary. However, the transition from variable to constant flowing enthalpy over a finite range of flowrates (fig. 5) should occur regardless of the relative-permeability functions used.

Useful extensions of this work might include 1) further sets of one-dimensional experiments that bring the constant pressure-enthalpy boundaries closer to the critical point (within 2°C); 2) simulations of the Dunn and Hardee (1981) experiments, with comparisons to the Cox and Pruess (1990) results; and 3) simulations of free convection within a vertical slab.

SUMMARY

The geothermal-modeling program GEOTHER2 is capable of simulating both multiphase flow and flow beyond the critical point. Extending the program to supercritical conditions was relatively straightforward because the governing equations are written in terms of pressure and enthalpy, which eliminates singularities at the critical point. Sets of one-dimensional experiments indicate that permeability is an important factor in determining pressure - enthalpy/temperature trajectories: low-permeability trajectories define a constant temperature gradient, whereas high-permeability trajectories maintain a constant flowing enthalpy. Further two-dimensional tests are needed to investigate the influence of the critical point on convective heat transfer and overall fluid-flow patterns.

ACKNOWLEDGMENTS

We would like to thank Cliff Voss, Mike Sorey, James Bischoff and an anonymous reviewer for their thoughtful criticisms. Their comments, especially on our numerical results, greatly improved this manuscript.

NOTATION

C_v = isochloric heat capacity
D = depth
g = gravitational acceleration
H = enthalpy
$\mathbf{k}$ = intrinsic permeability tensor
K_m = medium thermal conductivity-thermal dispersion coefficient
k_r = relative permeability ($0 \leq k_r \leq 1$)
P = pressure
R = mass source/sink flowrate
S = volumetric liquid saturation
T = temperature
t = time
ϕ = porosity
ρ = density
μ = dynamic viscosity
v = Darcian velocity (volumetric flowrate)

Subscripts
r refers to the porous medium (rock)
s refers to steam
w refers to liquid water

REFERENCES CITED

Battistelli, A., Calore, C., and Pruss, K., 1993, A fluid property module for the TOUGH2 simulator for saline brines and non-condensible gas: Eighteenth Stanford Geothermal Workshop, in press.

Bredehoeft, J.D., and Papadopolous, I.S., 1965, Rates of vertical ground water movement estimated from the Earth's thermal profile: Water Resources Research, v. 1, p. 325-328.

Cathles, L.M., 1977, An analysis of the cooling of intrusives by ground-water convection which includes boiling: Economic Geology, v. 72, p. 804-826.

Cox, B.L., and Pruess, Karsten, 1990, Numerical experiments on convective heat transfer in water-saturated porous media at near-critical conditions: Transport in Porous Media, v. 5, p. 299-323.

Dunn, J.C., and Hardee, H.C., 1981, Superconvecting geothermal zones: Journal of Volcanology and Geothermal Research, v. 11, p. 189-201.

Faust, C.R., and Mercer, J.W., 1977, Finite-difference model of two-dimensional, single- and two-phase heat transport in a porous medium-version I: U.S. Geological Survey Open-File Report 77-234, 84 p.

Faust, C.R., and Mercer, J.W., 1979a, Geothermal reservoir simulation 1. Mathematical models for liquid- and vapor- dominated hydrothermal systems: Water Resources Research, v. 15, p. 23-30.

Faust, C.R., and Mercer, J.W., 1979b, Geothermal reservoir simulation 2. Numerical solution techniques for liquid- and vapor-dominated hydrothermal systems: Water Resources Research, v. 15, p. 31-46.

Faust, C.R., and Mercer, J.W., 1982, Finite-difference model of three-dimensional, single- and two-phase heat transport in a porous medium, Scepter documentation and user's manual: Reston, Virginia, Geotrans, Inc., 73 p.

Haar, Lester, Gallagher, J.S., and Kell, G.S., 1984, NBS/NRC steam tables: thermodynamic and transport properties and computer programs for vapor and liquid states of water in SI units: New York, Hemisphere Publishing Corp., 320 p.

Hayba, D.O., 1993, Hydrologic modeling of the Creede epithermal ore-forming system, Colorado: Ph.D. thesis, University of Illinois, 186 p.

Ingebritsen, S.E., 1986, Vapor-dominated zones within hydrothermal convection systems: Evolution and natural state: Ph.D thesis, Stanford University, 179 p.

Johnson, J.W., and Norton, Denis, 1991, Critical phenomena in hydrothermal systems: state, thermodynamic, electrostatic, and transport properties of H_2O in the critical region: American Journal of Science, v. 291, p. 541-648.

Norton, Denis, and Knight, J., 1977, Transport phenomena in hydrothermal systems: cooling plutons: American Journal of Science, v. 277, p. 937-981.

Press, W.H., Flannery, B.P., Teukolsky, S.A., and Vetterling, W.T., 1986, Numerical recipes: the art of scientific computing: New York, Cambridge University Press, 818 p.

Pruess, Karsten, 1991, TOUGH2-A general-purpose numerical simulator for multiphase fluid and heat flow: Lawrence Berkeley Laboratory Report LBL-29400, 102 p.

Roberts, P.J., Lewis, R.W., Carradori, G., and Peano, A., 1987, An extension of the thermodynamic domain of a geothermal reservoir simulator: Transport in Porous Media, v. 2, p. 397-420.

Sengers, J.V., and Kamgar-Parsi, B., 1984, Representative equations for the viscosity of water substance: Journal of Physical and Chemical Reference Data, v. 13, p. 185-205.

Watson, J.T.R., Basu, R.S., and Sengers, J.V., 1980, An improved representative equation for the dynamic viscosity of water substance: Journal of Physical and Chemical Reference Data, v. 9, p. 1,255-1,290.